Pergamon

Cement and Concrete Research, Vol. 25, No. 5, pp. 1031-1042, 1995

0008-8846/95 $9.50+.00

0008-8846(95)00098-4

STUDY OF SHEAR FRACTURE IN MORTAR SPECIMENS

J. Davies
Department of Civil Engineering and Building,
The University of Glamorgan, Pontypridd CF37 1DL, UK

(Refereed)
(Received September 2; in final form October 26, 1994)

ABSTRACT

The Linear Elastic Finite Element Analysis was used to determine the influence of geometry and loading conditions on the stress distribution in specimens proposed for fracture testing in mixed mode loading. To establish the contribution of the shear part of the loading towards the overall cracking process, the stress intensity factors KI and KII at the notch tips were estimated from numerical displacements. It was established that in some cases KII is significantly higher than KI, indicating that the shear part of loading plays an important role during the fracture process. The numerical study was complemented by a series of experiments which indicated that shear fracture can be generated if the symmetry of specimen geometry and loading is maintained. A comparison of fracture zone characteristics generated under static and impact loading is also given and it was observed that the strain rate does not alter the fundamental features of a cracking process.

Introduction

Linear elastic fracture mechanics (LEFM) is the study of stresses and displacements fields near a crack tip in an isotropic, homogeneous elastic material at the onset of rapid, unstable crack propagation which leads to fracture. This theory provides a means of predicting the fracture stress of structural components containing flaws or cracks of known size and location in terms of stress intensity factor K. The factor K is a parameter which depends on applied stress, crack length and dimensions of the specimen. Thus K is a measure of the properties of the material when a crack is present and has dimensions of stress x (length)$^{-1/2}$. The usual units are MN m$^{-3/2}$. The generalised equation

describing the stress field in the vicinity of crack tip may be written as

$$\sigma = K(2\pi r)^{-1/2} f(\theta) \qquad (1)$$

where r is the distance from the crack tip, σ the applied stress K the stress intensity factor and is f(θ) Westergaard's function. In Fracture Mechanics, there are three basic modes of crack propagation,FIG.1.

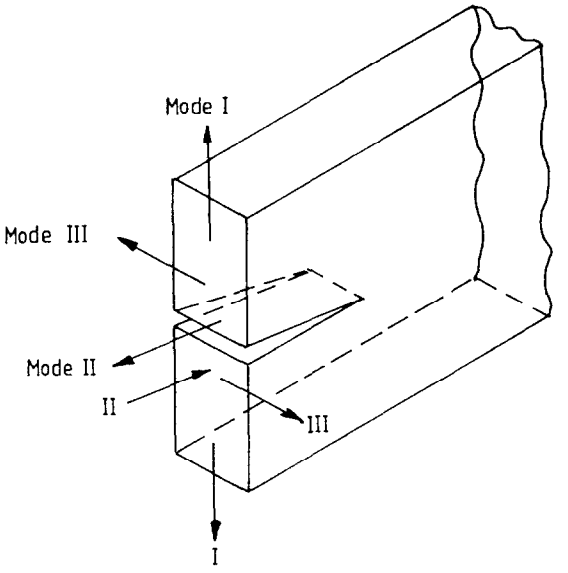

FIG. 1.
Basic Modes of Failure

(1) Mode I or opening mode is associated with crack surface displacements normal to the crack plane
(2) Mode II or edge sliding mode is associated with crack surface displacements in the crack plane and normal to the crack face
(3) Mode III or tearing mode is associated with crack surface displacements in the crack plane and parallel to the crack face

The superposition of these three modes is sufficient to describe the most general case of crack tip deformation and stress field. The stress intensity factors associated with each mode of failure are assigned KI, KII and KIII respectively.

Most of the fracture studies and tests developed have concentrated on Mode I (tensile) type of failure . The growing interest in the specimen geometry suitable for materials fracture testing in Mode II (in-plane shear), resulted in more active research in both experimental and analytical fields of analyses (1-6), but there is still a lack of experimental and analytical data on this potentially significant mode of failure. The purpose of this investigation is to improve the understanding of Mixed Mode fracture process and to clarify the basis that can be used to describe the crack propagation under shear compression loading.

The punch-through shear cube specimens with asymmetrical notches were studied using both Finite Element Analysis and experiments, and an assessment was made as to their suitability for fracture testing in shear compression. The main objective of the numerical analysis was to determine stress distributions in the ligament containing a notch together with the stress intensity factors KI and KII at the notch.

FIG.2. shows the geometry of the cube specimens together with the appropriate notation. The cubes were based on the standard 100mm concrete cube geometry and modified with a series of opposite notches; the top notches being kept constant at 10mm and the bottom notches varied from a = 25mm to 60mm in 5mm increments. The notches were inserted by means of a 'Clipper' masonry saw fitted with a 253 mm diamond steel blade producing 2mm wide notches. The matrix composition of the mortar was 1:3: 0.45 (c:s:w) and its quality was carefully maintained throughout the experimental programme. The specimens were stripped after 24 hours and cured in water at a constant temperature of 22°C for 28 days. Tests were performed in the displacement control mode of an Instron 1251 testing machine fitted with purpose made Instron compressive platens. The cross head speed was kept constant throughout the programme at the rate of 0.003mm/s.

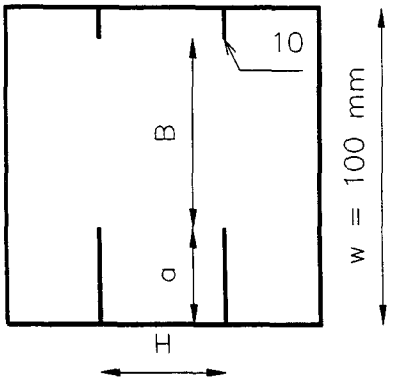

H (mm)
50
40
30

FIG.2.
Geometry of punch-through shear specimen

Results

Finite Element Analysis

Many approximate solution procedures have been developed for the analysis of fracture problems because of the difficulties involved in obtaining an analytical solution, even for simple geometries and loading systems.

It has been shown that a high degree of mesh refinement is required to obtain acceptable solutions and that the accuracy of the solution varies greatly with the size and shape of the elements and with the general configuration of the mesh. The accu-

racy of the finite element analysis has been largely improved by using isoparametric finite elements which are also suitable for application to cracked bodies. These elements are available in most general purpose computer programs and they satisfy convergence criteria, inter-element compatibitlity, constant strain modes, continuity of displacements and rigid body motion.

The accuracy of the solution of fracture problems varies with the method of computing the stress intensity factors. The commonly used linear extrapolation methods (stress or displacement) requires a large number of elements in order to achieve acceptable solution accuracy and consequently increase the cost of computer analysis. The conic section simulation method reported by Woo and Kuruppu (7) enables one to compute the stress intensity factor directly from the results obtained from Finite Element Analysis. The method makes use of the technique of mapping the the nodal displacement of the crack surface into an elliptical displacement function and the expression for the stress intensity factors KI and KII are given as

$$K_I = \frac{u(x,0)\,E}{(1-\frac{x^2}{a^2})^{1/2}\,2a}\,(\pi a)^{1/2} \qquad (2)$$

and

$$K_{II} = \frac{v(x,0)\,E}{(1-\frac{x^2}{a^2})^{1/2}\,2a}\,(\pi a)^{1/2} \qquad (3)$$

where u(x,0) and v(x,0) are nodal displacements obtained from finite element solution, 'a' is a crack length, E the modulus of elasticity and x the distance ahead of a crack.

The finite element code used in this research programme was PAFEC-FE interactive system together with PIGS 4.1 suite which run on VAX 11/785 mini-computer. The geometry of a numerical model, assumed boundary conditions and the finite element mesh are shown in FIG.3.

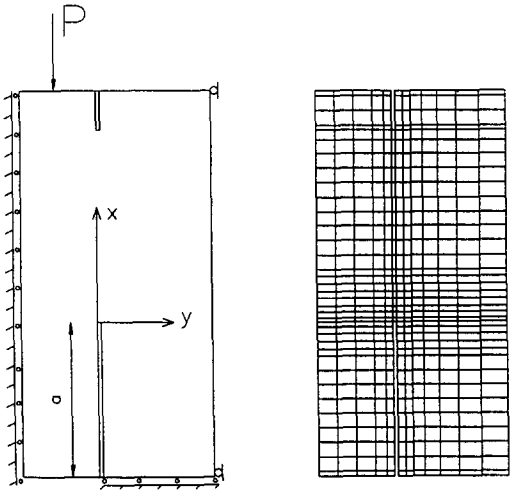

FIG.3.
Boundary conditions and finite element mesh

Due to the symmetry only one half of the specimen was modelled. A compressive load was applied through the 'repeated freedom' module which simulates partially distributed load with sufficient accuracy. Typical results obtained from the stress analysis are presented for a 100 mm cube with a=40 mm and H = 30 mm (for notation see FIG.2.), where 640 isoparametric elements were used. The smallest element size generated in the notch region was in the order of 0.02a. The line of symmetry and the supports were represented by a series of rollers as shown in FIG. 3.

It has been stated by many investigators that the brittle fracture in compression is due to tensile microstresses, however the tensile mechanism is not in itself sufficient to cause failure. Another failure mechanism, most probably controlled by shear stresses, becomes active at some stage of the fracture process. FIG.4 is a typical plot of in-plane shear and maximum shear stresses in the specimen. It should be remembered that the values of stress levels in the notch region are approximate and therefore should be taken as an indication of the order of magnitude and not as values from which the failure loads may be predicted.

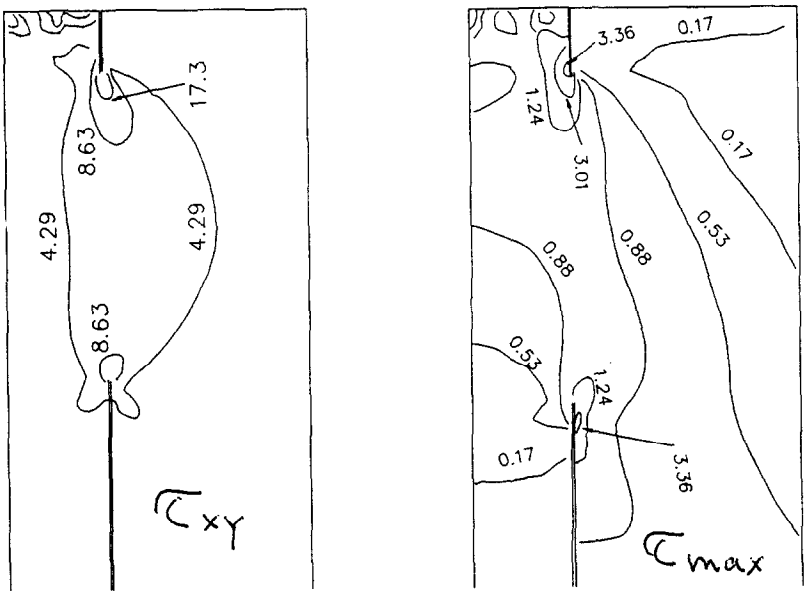

FIG.4.
Variation of in-plane and maximum shear stresses

In order to investigate whether this test arrangement maximizes the Mode II failure mechanism, the stress intensity factors KI and KII were evaluated using equations 2 and 3. Extensive analyses were carried out on specimens subjected to the unity load with varying H/w and a/w aspect ratios (4,8) and it was found that with decreasing H/w ratio the shear part of loading assumes a greater significance. TABLE 1 gives a summary of estimates of KI and KII stress intensity factors together with KI/KII ratios. For the specimen discussed here with H = 30mm and a/w = 0.4 the KII/KI ratio was found to be in the order of 30, the result indicating predominance of Mode II (shear) type of failure. Experimental values of KII reported by the author in (2) were found in the order of 2.09 $MNm^{-3/2}$. It was also observed that the initial crack evolution begins at about 40% of the load when the main fracture zone has formed, see FIG.10. Some investigators (9) suggested that shear fracture is not possible and that the failure mechanism of components loaded in shear is always initiated by tensile stresses (Mode I).

TABLE 1
Estimates of KI, KII and KII/KI Ratios for 100mm Model

a/W	H = 50mm			H = 40mm			H = 30mm		
	K_{II} ($Nmm^{-3/2}$)	K_I ($Nmm^{-3/2}$)	K_{II}/K_I	K_{II} ($Nmm^{-3/2}$)	K_I ($Nmm^{-3/2}$)	K_{II}/K_I	K_{II} ($Nmm^{-3/2}$)	K_I ($Nmm^{-3/2}$)	K_{II}/K_I
0.25	2.141	0.216	9.9	1.839	0.185	9.9	1.590	0.132	12.0
0.30	2.329	0.214	10.9	1.993	0.170	11.7	1.773	0.114	15.2
0.35	2.468	0.198	12.5	2.142	0.152	14.1	1.860	0.093	20.0
0.40	2.656	0.169	15.7	2.280	0.124	18.4	1.972	0.066	29.9
0.45	2.786	0.162	17.2	2.416	0.112	21.6	2.085	0.054	38.6
0.50	2.820	0.148	19.1	2.500	0.078	32.1	2.120	0.031	68.4
0.55	3.050	0.118	25.8	2.620	0.065	40.3	2.300	0.021	109.5
0.60	3.250	0.104	31.3	2.820	0.060	47.0	2.480	0.020	124.0

Experimental investigation.

To investigate these statements and to study the crack characteristics in shear compression field, numerous experiments have been performed on modified mortar cubes as described above. The monitoring of the fracture zone formation was carried out with the aid of a video camera having the fast shutter speed, 500 - 1000 frames/sec. It was possible to split the cracking process into frames 1/25sec appart and to study the formation and the crack propagation on a macroscopic basis (10,11).

Photographs presented in this paper indicate typical types of failure mechanisms observed in the tested specimens. A set of photographs, FIG.5, shows a band of discontinuous cracks which is formed in the ligament of a punch-through shear cube, without any apparent tensile cracks emanating simultaneously from both notches. With increasing load, the cracks grow in number from various locations between two slots, and finally produce a narrow crush zone.

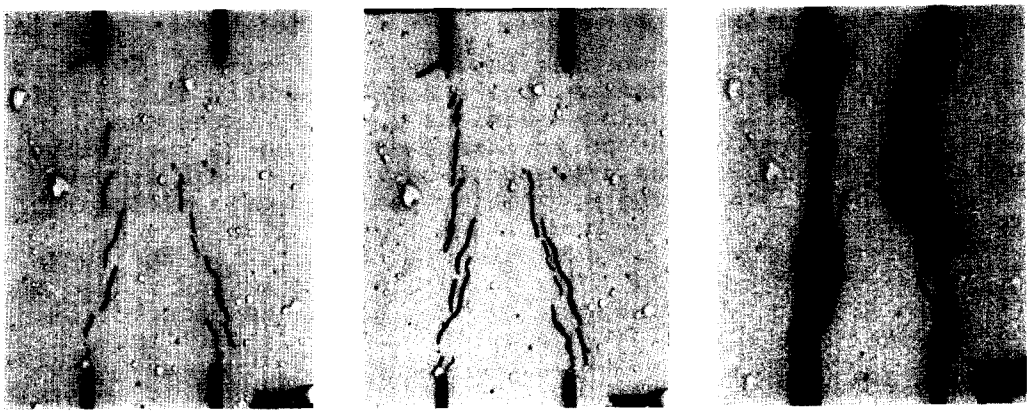

Initial fracture Final fracture

FIG.5.
A fracture zone development in a punch-through shear cube

The accurate insertion of notches is the vitally important factor affecting the fracture path development and its characteristics. FIG.6a,b,c,d shows an inclined tensile crack starting from one notch together with a faint band of discontinuous multiple cracks appearing within the ligament. In this case the symmetry of notch geometry was violated by inserting one notch 1 mm shorter than required.

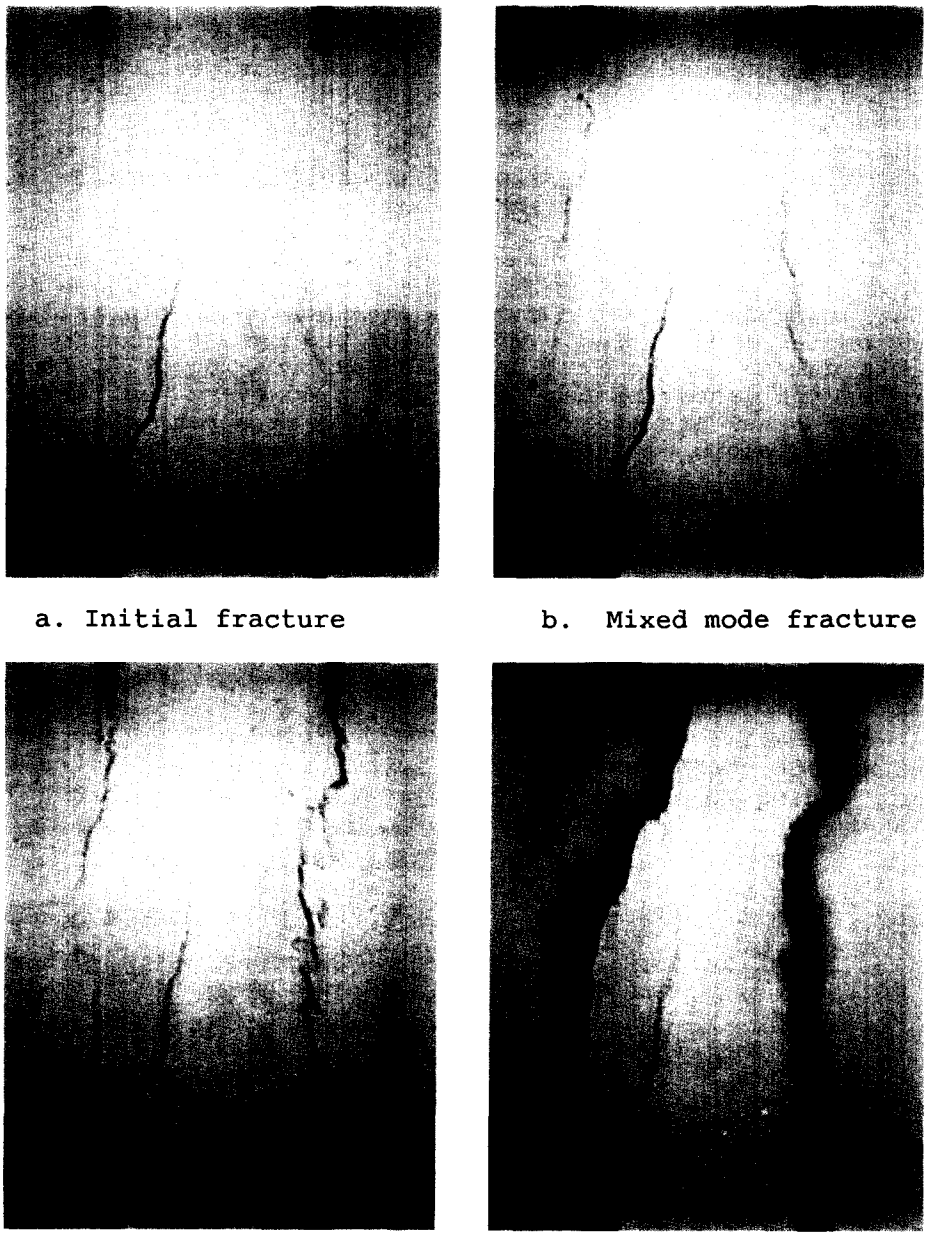

a. Initial fracture

b. Mixed mode fracture

c. Crushing of crack face bridges

d. Final fracture

FIG.6.
Mapping of tensile and shear cracks within the ligament.

However, it can be clearly seen that despite this initial tensile crack, the progressive discontinuous fissures are jointed by small compressive struts indicating shear transfer by aggregate interlock. FIG 6c. shows the crack path formation a fraction of a second before the failure, and FIG.6d was taken at the instant of a complete fracture. The initial tensile crack (Mode I) is not extending with increasing load, and the final crush zone is considerably narrower than that in the previous case.

A careful study of FIGs.5 and 6 revealed that the gaps in the failure zone, called material or crack face bridges, appeared to be of a different nature. It was observed, that the extent and distribution of the crack face bridges will depend on the type of failure mechanism which was most likely predominant during the cracking process. It would appear that the crush zone in cubes was wider if the Mode II failure mechanism was maximized from the onset of the fracture process and the narrower crush zone was observed in specimens with some subcritical tensile crack appearing in the ligament. The way that the bridges were finally damaged might also indicate the most probable failure mechanism involved during the cracking process. It can be said that the damage to the bridges caused by crushing, FIG. 6c, indicates that shearing has taken place. However, when the two overlaping crack branches finally reach each other, the dominant failure mode would be the opening tensile mode, Mode I.

FIG.7. shows another example of failure obtained from the punch-through shear cubes. In this case, the symmetry of the specimen was violated by the insertion of notches which were not parallel. The combination of tensile (inclined) cracks and a vertical crush zone produced by the interaction and linkage of a distributed array of microcracks clearly indicates that two different failure mechanisms were activated during the fracturing process, namely tensile and shear.

In order to examine the effect of the strain rate on the fracture path characteristics the specimens were subjected to impact loading in square wave mode of amplitude 5 mm and 0.1 Hz frequency.

FIG.7.
Mixed-Mode failure of punch-through shear cube

FIG.8.shows the characteristics of the fracture zone resulting from the impact tests on perfectly symmetrical cubes. The cracks are parallel with the direction of maximum shear stresses and more significantly, no subcritical tensile cracks can be traced. However, FIG.9 shows a cube with the imperfect geometry (notches of different depths) where a subcritical tensile crack emanated from one notch. There is a remarkable similarity with the situation reported in FIG.6.

A comparison of static (displacement controlled) and impact tests clearly indicated that the symmetry of both loading and the specimen geometry is the paramount factor which maximizes Mode II fracture. It was further observed that in the static tests the crack growth was fairly stable, see FIG.10, until the density of microcracks defined the fundamental fracture path which was parallel with the direction of maximum shear planes. This was followed by the rapid final fracture which was in some cases almost explosive. Such behaviour could be attributed to the frictional interlocking and bridging between the array of

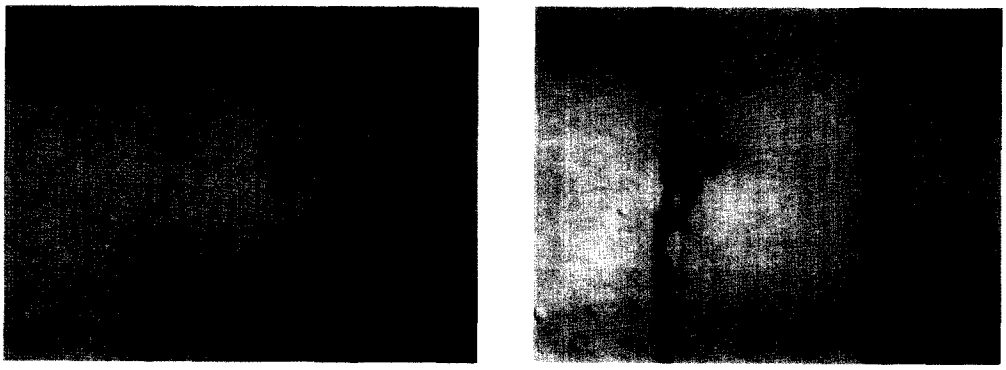

FIG.8.
Impact failure of a 'perfect' cube

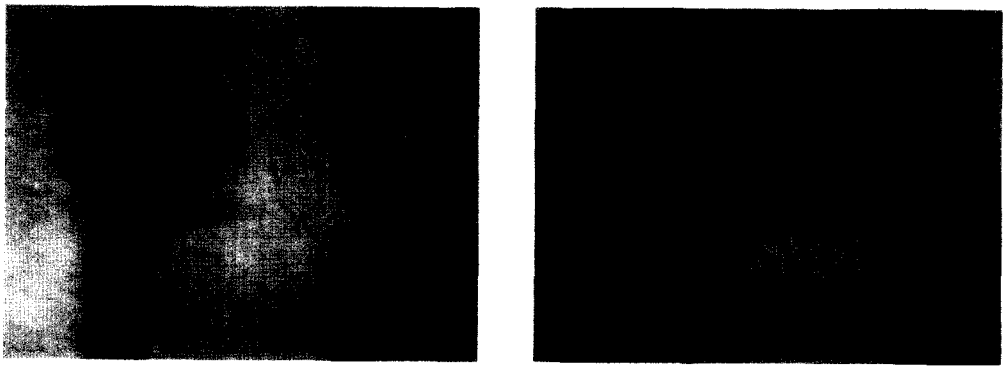

FIG.9.
Impact failure of an 'imperfect' cube

adjacent crack faces. This activity would cause a gradual build up and then a sudden release of the stored energy. The absence of the inclined (tensile) cracks as demonstrated in the symmetrical specimens is the basic characteristic which the author associates with shear fracture.

FIG. 10 is an example of typical load-deflection curves obtained from the experiments. The first crack load was found to be in order of about 40% of the maximum load. At this stage, in the 'perfect' cube, the discontinuous cracks appeared simultaneously as shown in FIG.5. In the 'imperfect'cube, however, the inclined crack appeared firstly followed by the band of discontinuous cracks as demonstrated in FIG.6. In both cases the progressive cracking together with crushing of the crack face bridges took place between the first crack load and the maximum load, (the cracking process was fairly stable). After the maximum load was reached the fracture process become unstable and very fast.

The discontinuous nature of the fracture zone also demonstrates that the fracture in cementitious materials is initiated when stresses over a fracture process zone reach a critical value, rather than their value at some point as it is in the case of homogeneous and elastic materials. Another reason for this may be the fact, that cementitious materials have a variable

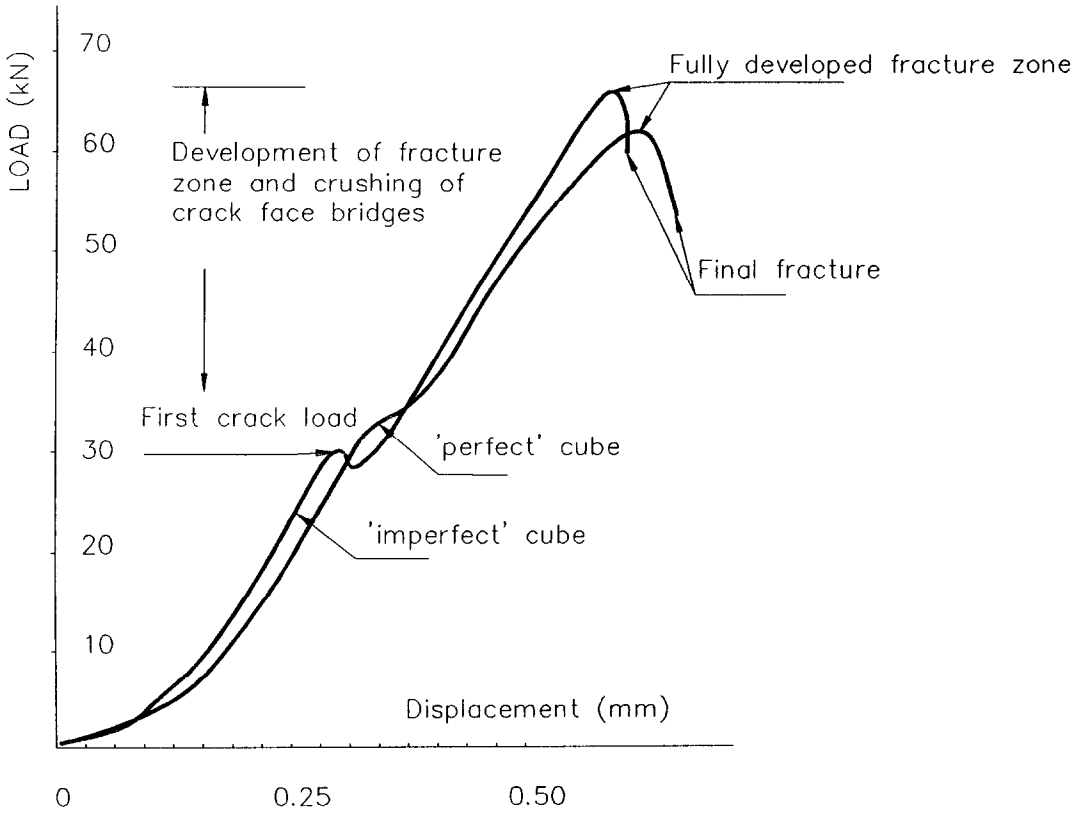

FIG.10.
Load - displacement curves for 'perfect' and 'imperfect' cubes

strength throughout their bodies and consequently "low strength zones" coupled with a high stress concentration will be the potential failure planes.

Summary and conclusion

- Finite element analysis was used to study the stress distribution and the LEFM approach was used to perform the fracture mechanics analysis. It was determined that the stress intensity factor KII associated with the shear part of a loading component was predominant indicating that a mixed mode of failure with the significant shear component could be generated.

- Experiments conducted on 100 mm mortar cubes prepared for the punch-through shear tests showed that the crack path consisted of a series of microfissures which emanated from both notches and which were separated by the crack face bridges. It is suggested that the distibution and damage of the crack face bridges could be related to the type of failure mechanism which governs the cracking process. The crack face bridges damaged by crushing and finally producing a narrow crush zone could be attributed to a shear failure (Mode II) . However, the crack face bridges which overlap and produce a seemingly continuous single crack could be attributed to a tensile failure (Mode I).

- A comparison of fracture characteristics associated with the static and impact tests showed that in both cases cracks were discontinuous microfissures which formed predominantly in the vertical or almost vertical direction within a ligament containing the top and bottom notches when both the symmetry of loading and the specimen geometry were achieved.

When the symmetry of the system was violated, the action of high shear force concentration also generated fracture mechanism with cracks propagating in the direction of maximum shear planes. However a subcritical tensile crack emanating from one of the notches signalled the presence of the Mode I. As can be seen this tensile crack did not open during subsequent loading indicating that the tensile fracture does not contribute to the final shearing process.

- Experimental observations lead to the conclusion that the shear fracture could be generated in punch-through shear cubes which are perfectly symmetrical and that the stain rate does not alter the fundamental elements of the shear fracture. This major limitation may be the prime reason why so many researchers argue that shear fracture does not exist.

- The macroscopic fracture studies provide an important aid for engineers in design against fracture in actual structures. It is of great importance to know the relationship between the load at which the initiation of microcracking begins and the load at which the main crack forms. In the presented study it was observed that the initial signs of cracking appeared at a load which was about 40% of the load when the main fracture zone has

formed. This microcrack damage development may be regarded as a mechanism of fracture toughness enhancement, a similar phenomenon that is observed in ductile alloys. The results reported here are not necessarily applicable to other types of geometries and loading combinations.

Acknowledgements

The author wishes to express her gratitude for invaluable help and support given by the staff of Media Resources unit at the University of Glamorgan, namely Viv Cole, Chris Thomas, Malcom Coundley and John Adams.

References

1. Bazant,Z.P and Pfeiffer,P., Materials and Structures,(RILEM) 19, 110, p.111,(1986)
2. Davies,J., Yim,CWA, Morgan TG., Int. J. Cem. Com., Volume 9, No.1, p.33 (1987)
3. Van Mier, J.G.M.,Fracture processes in concrete, rock and ceramics, Vol.I, p.27, Chapman and Hall, (1991)
4. Davies,J., Int. J. Cem.Comp., 10, p. 3. (1988)
5. Luong, M.P, Fracture processes in concrete, rocks and ceramics Vol. II, p. 727, (1991)
6. Van Mier,J.G.M,Schlangen E.,Nooru-Mohamed M.B.,Fracture mech. of concrete struct. Elsevier Appl. Science, p.659,(1992)
7. Woo,C.W. and Kuruppu M.D., Int. Jr.of Fracture, Vol.20, p.63, 1982.
8. Yim,C.W.A, M.Phil. Thesis, CNAA,London, 1986.
9. Ingraffea,A.R. and Panthaki,N.I., ed. C.Meyer & H.Okamura, ASCE, New York, p.151, (1985)
10. Davies,J., Fracture processes in concrete, rocks and ceramics Vol. II. p. 717, Chapman and Hall, (1991)
11. Davies, J., Fracture machanics of concrete structures, p. 713 Elsevier Applied Science, (1992)